Supporting Information for "Including filter-feeding gelatinous macrozooplankton in a global marine biogeochemical model: model-data comparison and impact on the ocean carbon cycle"

C. Clerc[1] *, L. Bopp[1], F. Benedetti [2], M. Vogt [2], and O. Aumont[3]

Corentin Clerc et al.

[1]LMD / IPSL, Ecole normale supérieure / Université PSL, CNRS, Ecole Polytechnique, Sorbonne Université, Paris, France

[3]LOCEAN / IPSL, IRD, CNRS, Sorbonne Université, MNHN, Paris, France

[2]Environmental Physics, Institute of Biogeochemistry and Pollutant Dynamics, ETH Zürich, 8092, Zürich, Switzerland.

Contents of this file

Text S1.

Nutrients and Oxygen: Map a. (resp. b.) in Fig. S2 presents the observed (resp. simulated) surface concentrations of nitrates. The model performs particularly well for

*corentin.clerc -at- lmd.ens.fr

https://orcid.org/0000-0002-8436-4391

surface nitrates, with absolute values and simulated spatial patterns very consistent with observations (r=0.83). The model performance is very similar for phosphates (r=0.83) and sub-surface oxygen (r=0.92). For bottom oxygen (2000-4000 m, not shown), performance is reduced, with a Pearson correlation coefficient of only 0.35. Too much oxygen seems to accumulate at the bottom (bias = +52 mmol m^{-3}).

Chlorophyll: The modeled annual chlorophyll distribution is compared to OC-CCI satellite observations in Fig. S2 c. and d. The correspondence between the observed and simulated surface chlorophyll is rather satisfactory (r= 0.59). The average value is similar (0.37 vs 0.42 mgChl m^{-3}) and the spatial structure is respected overall. The overall variability is of the same order of magnitude in the model and the observations (standard deviation of 0.32 mmol $m^{-3}$for the model and 0.64 mmol m^{-3} for the observations). However, there are some differences. At high latitudes, particularly in the Southern Ocean, the model tends to overestimate the chlorophyll compared to the satellite product. However, satellite chlorophyll may be underestimated by a factor of about 2 to 2.5 by the algorithms deducing chlorophyll concentrations from reflectance as discussed in (Aumont et al., 2015).

Mesozooplankton: Mesozooplankton annual distribution on the top 300 m is compared to the MAREDAT product in Fig. S2 e. and f. The model performs quite well (r=0.45) and fits the observed spatial patterns, and the distribution of high vs low concentration regions. However, it tends to overestimate the low concentrations and underestimate the high concentrations. Indeed, mesozooplankton variability is slightly reduced in the model (standard deviation of 0.34 vs 0.59 mmol C m^{-3} in the observation).

Text S2.

Macrozooplankton dynamics: :

G_X, the ingested matter, is depending on food availability to X. We distinguish two predation behaviours: concentration-dependent grazing and flux feeding.

Concentration-dependent grazing is based on a Michaelis-Menten parameterization with no switching and a threshold (Gentleman et al., 2003). The equation describing the grazing rate of X on prey I, $g^X(I)$, is derived as:

$$F^X = \sum_J p_J^X \max\left(0, J - J^X_{\text{thresh}}\right) \tag{S1}$$

$$F^X_{\text{lim}} = \max\left(0, F^X - \min\left(0.5F, F^X_{\text{thresh}}\right)\right) \tag{S2}$$

$$g^X(I) = g^X_m \frac{F_{\text{lim}}}{F} \frac{p_I^X \max\left(0, I - I^X_{\text{thresh}}\right)}{K_G^X + \sum_J p_J^X J} \tag{S3}$$

where F^X is the available food to X, g^X_m is the maximal grazing by X rate, F^X_{thresh} is the feeding threshold for X, I^X_{thresh} is the group I threshold for X, K_G^X is the half saturation constant for grazing by X, p_I^X is the X preference for group I.

Flux-feeding accounts for particles traps deployed by some zooplankton species (Jackson, 1993). It is derived as a particles flux depending term, an thus depends on the product of the concentration by the sinking speed:

$$\text{ff}^X(I) = \text{ff}^X_m w_I I \tag{S4}$$

where $\text{ff}^H(I)$ is the flux-feeding rate of prey X on particle I, $\text{ff}^H(I)$ is the maximal flux-feeding rate of prey X on particle I, w_I is the vertical sinking velocity of I particles.

For GM:

$$G^{g}_{GM} = g^{GM}(P) + g^{GM}(D) + g^{GM}(\text{sPOC}) + g^{GM}(\text{bPOC}) + g^{GM}(Z) + g^{GM}(M) \quad \text{(S5)}$$

$$G^{\text{maxff}}_{GM} = \text{ff}^{GM}(\text{bPOC}) + \text{ff}^{GM}(\text{sPOC}) + \text{ff}^{GM}(Ca_{GM}) + \text{ff}^{GM}(Fp_{GM}) + \text{ff}^{GM}(Ca_{FFGM}) + \text{ff}^{GM}(Fp_{FFGM}) \quad \text{(S6)}$$

$$E^{\text{ff}}_{GM} = \frac{G^{\text{maxff}}_{GM}}{G^{g}_{GM} + G^{\text{maxff}}_{GM}} \quad \text{(S7)}$$

$$G^{\text{ff}}_{GM} = G^{\text{maxff}}_{GM} E^{\text{ff}}_{GM} \quad \text{(S8)}$$

$$G^{GM} = G^{\text{ff}}_{GM} + G^{g}_{GM} \quad \text{(S9)}$$

$$p^{GM}_{M} >> p^{GM}_{D} = p^{GM}_{Z} \quad \text{(S10)}$$

with E^{ff}_{GM} the proportion of filter-feeders, G^{maxff}_{GM} the potential ingestion by flux feeding,G^{ff}_{GM} the actual ingestion by flux feeding , G^{g}_{GM} the ingestion by concentration dependent grazing and p^{X}_{Y} the X preference for group Y

For FFGM:

$$G_{FFGM} = g^{FFGM}(P) + g^{FFGM}(D) + g^{FFGM}(\text{POC}) + g^{FFGM}(\text{GOC}) + g^{FFGM}(Z) + g^{FFGM}(M) \quad \text{(S11)}$$

$$p^{FFGM}_{D} = p^{FFGM}_{N}, p^{FFGM}_{Z} \quad \text{(S12)}$$

For the PISCES-CLG experiment (with FFGM clogging) run, the ingested matter by FFGM G^{CLG}_{FFGM} is:

$$G^{CLG}_{FFGM} = G_{FFGM} \times F_C(Chl) \tag{S13}$$

where $F_C(Chl)$ is the clogging function presented in Eq. 4 of the paper.

Carcasses dynamics: : Carcasses production by organisms X ($=FFGM$ or $=GM$) comes from non predatory quadratic and linear X mortalities. Loss terms include a temperature dependent term representing remineralization by saprophagous organisms and flux-feeding by GM. Flux feeding includes two terms : the ingested food by GM which is temperature dependent and the non ingested matter fractionated by flux feeding process (Dilling & Alldredge, 2000), which is assumed to be equal to the ingested portion except the temperature dependency.

$$\begin{aligned}\frac{\partial Ca_X}{\partial t} + w_{Ca_X}\frac{\partial Ca_X}{\partial z} &= m_c^X f_X(T)\left(1-\Delta(O_2)\right)X^2 \\ &+ r^X f_X(T)\left(\tfrac{X}{K_m+X} + 3\Delta(O_2)\right)X \\ &- E^{\text{ff}}_{GM}\text{ff}^{GM}(Ca_X)\left(1-\Delta(O_2)\right)f_{GM}(T)GM \\ &- E^{\text{ff}}_{GM}\text{ff}^{GM}(Ca_X)GM \\ &- \alpha f_\alpha(T)Ca_X\end{aligned} \tag{S14}$$

Where α is the remineralization rate.

Fecal pellets dynamics: :

Fecal pellets production by organisms X ($=FFGM$ or $=GM$) comes from non assimilated food. Loss terms, similarly to carcasses, include a temperature dependent remineralization term and a flux-feeding by GM term.

$$\begin{aligned}\frac{\partial Fp_X}{\partial t} + w_{Fp_X}\frac{\partial Fp_X}{\partial z} &= a^X I_X^g \left(1-\Delta(O_2)\right) f_X(T) X \\ &- E_{GM}^{\text{ff}} \text{ff}^{GM}(Fp_X)\left(1-\Delta(O_2)\right) f_{GM}(T) GM \\ &- E_{GM}^{\text{ff}} \text{ff}^{GM}(Fp_X) GM \\ &- \alpha f_\alpha(T) Fp_X \end{aligned} \tag{S15}$$

Where a^X is the X assimilation rate.

References

Aumont, O., Ethé, C., Tagliabue, A., Bopp, L., & Gehlen, M. (2015). PISCES-v2: An ocean biogeochemical model for carbon and ecosystem studies. *Geoscientific Model Development*, *8*(8), 2465–2513. doi: 10.5194/gmd-8-2465-2015

Dilling, L., & Alldredge, A. L. (2000). Fragmentation of marine snow by swimming macrozooplankton: A new process impacting carbon cycling in the sea. *Deep Sea Research Part I: Oceanographic Research Papers*, *47*(7), 1227–1245.

Garcia, H., Weathers, K., Paver, C., Smolyar, I., Boyer, T., Locarnini, M., ... others (2019). World ocean atlas 2018. vol. 4: Dissolved inorganic nutrients (phosphate, nitrate and nitrate+ nitrite, silicate).

Gentleman, W., Leising, A., Frost, B., Strom, S., & Murray, J. (2003). Functional responses for zooplankton feeding on multiple resources: a review of assumptions and biological dynamics. *Deep-Sea Research II*, *50*, 2847–2875.

Jackson, G. A. (1993). Flux feeding as a mechanism for zooplankton grazing and its implications for vertical particulate flux 1. *Limnology and Oceanography*, *38*(6), 1328–1331.

Kiørboe, T. (2013). Zooplankton body composition. *Limnology and Oceanography*, *58*(5), 1843–1850.

Lucas, C. H., Jones, D. O., Hollyhead, C. J., Condon, R. H., Duarte, C. M., Graham, W. M., ... Regetz, J. (2014). Gelatinous zooplankton biomass in the global oceans: geographic variation and environmental drivers. *Global Ecology and Biogeography*, *23*(7), 701–714.

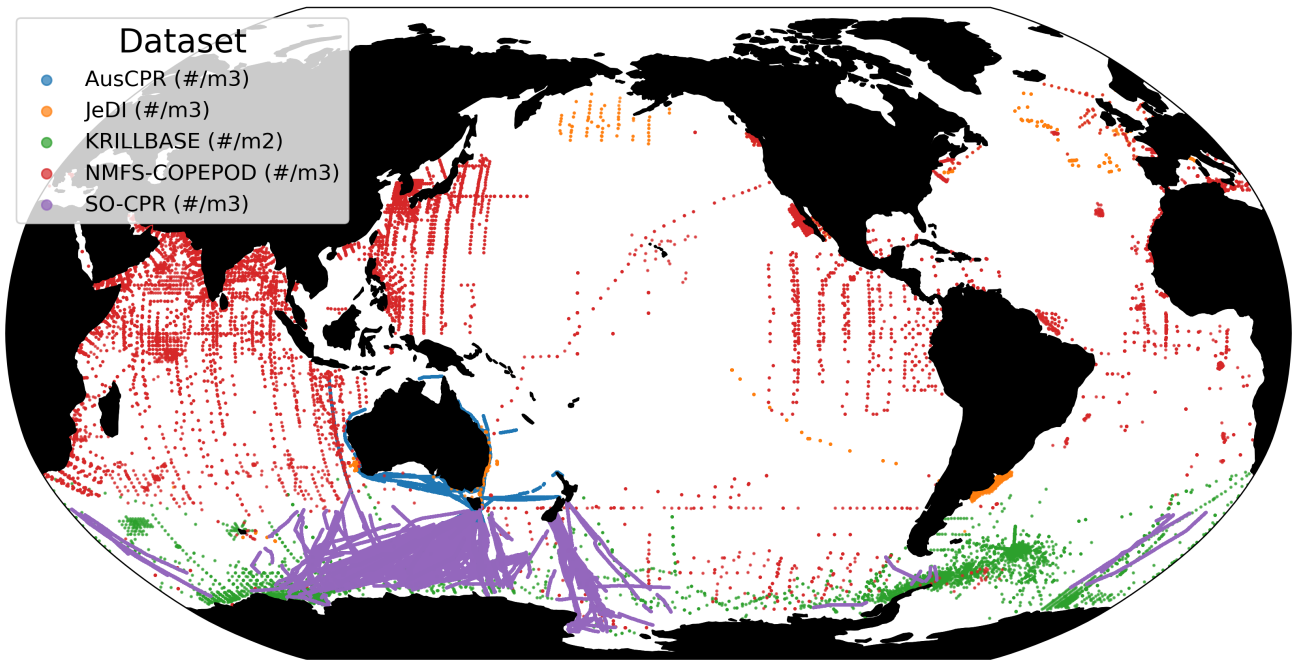

Figure S1. Map of the FFGM observations in the AtlanECO product. Colors indicate the original dataset.

Class	Order	Genus	Species	Individual weight (mg C ind^{-1})	Source
Thaliacea	Doliolida	*Dolioletta*	*gegenbauri*	0.0192	(Lucas et al., 2014)
Thaliacea	Pryosomatida	*Pryosoma*	*atlanticum*	22.9036	(Lucas et al., 2014)
Thaliacea	Salpida	*Brooksia*	*rostrata*	0.0019	(Lucas et al., 2014)
Thaliacea	Salpida	*Cyclosalpa*	*affinis*	2.8196	(Lucas et al., 2014)
Thaliacea	Salpida	*Cyclosalpa*	*bakeri*	4.7948	(Lucas et al., 2014)
Thaliacea	Salpida	*Cyclosalpa*	*floridana*	0.1146	(Lucas et al., 2014)
Thaliacea	Salpida	*Cyclosalpa*	*pinnata*	3.473	(Lucas et al., 2014)
Thaliacea	Salpida	*Cyclosalpa*	*polae*	0.5262	(Lucas et al., 2014)
Thaliacea	Salpida	*Iasis*	*zonaria*	3.9887	(Lucas et al., 2014)
Thaliacea	Salpida	*Ihlea*	*punctata*	0.1673	(Lucas et al., 2014)
Thaliacea	Salpida	*Pegea*	*bicaudata*	7.9575	(Lucas et al., 2014)
Thaliacea	Salpida	*Pegea*	*confoederata*	1.8974	(Lucas et al., 2014)
Thaliacea	Salpida	*Pegea*	*socia*	1.6717	(Lucas et al., 2014)
Thaliacea	Salpida	*Salpa*	*aspera*	2.9474	(Lucas et al., 2014)
Thaliacea	Salpida	*Salpa*	*cylindrica*	0.56	(Lucas et al., 2014)
Thaliacea	Salpida	*Salpa*	*fusiformis*	1.33	(Lucas et al., 2014)
Thaliacea	Salpida	*Salpa*	*maxima*	3.2305	(Lucas et al., 2014)
Thaliacea	Salpida	*Thalia*	*democratica*	0.042	(Lucas et al., 2014)
Thaliacea	Salpida	*Thetys*	*vagina*	0.404	(Lucas et al., 2014)
Thaliacea	Salpida	*Salpa*	*thompsoni*	10.57	(Kiørboe, 2013)

Table S1. Table of individual weights used for abundance to biomass conversions For *Salpa thompsoni*, we computed the mean of the corresponding mass measurements of individual zooplankters in table A1 of Kiørboe (2013). For all the other species, we used values from Appendix S4 from Lucas et al. (2014)

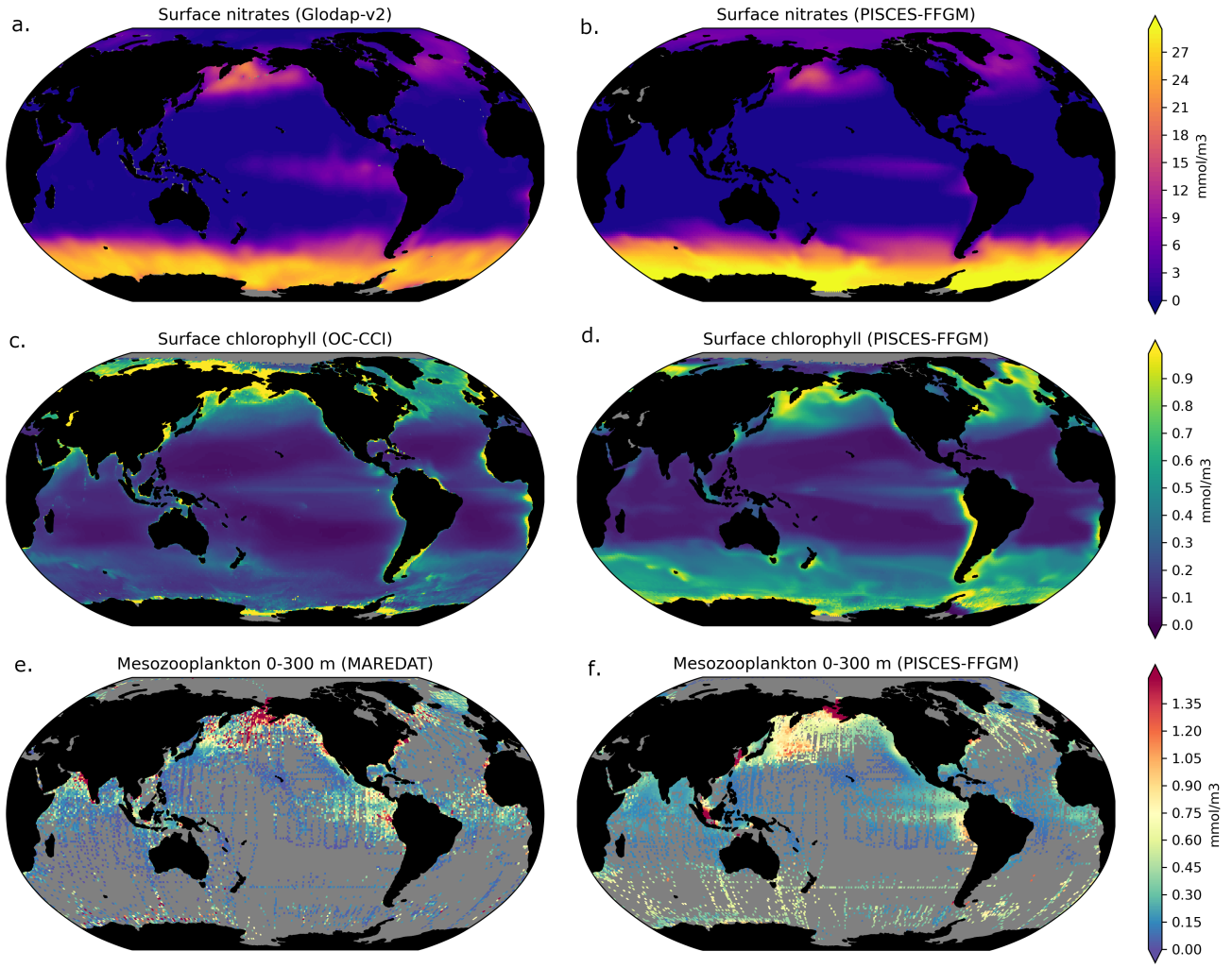

Figure S2. Comparison between modeled and observed surface ntirates, surface chlorophyll and top 300m mesozooplankton. a. Annual average Glodap-v2 surface nitrates concentration interpolated from observation on 1 degree grid. f. Annual average modeled nitrates concentrations on 1 degree grid. c. Annual average of monthly OC-CCI surface chlorophyll concentration on 1 degree grid. d. Annual average of monthly modeled surface chlorophyll concentrations on 1 degree grid masked for missing monthly observations. e. Annual average of monthly MAREDAT top 100m mesozooplankton concentration observations on 1 degree grid. f. Annual average of monthly modeled mesozooplankton concentrations on 1 degree grid masked for missing monthly observations.

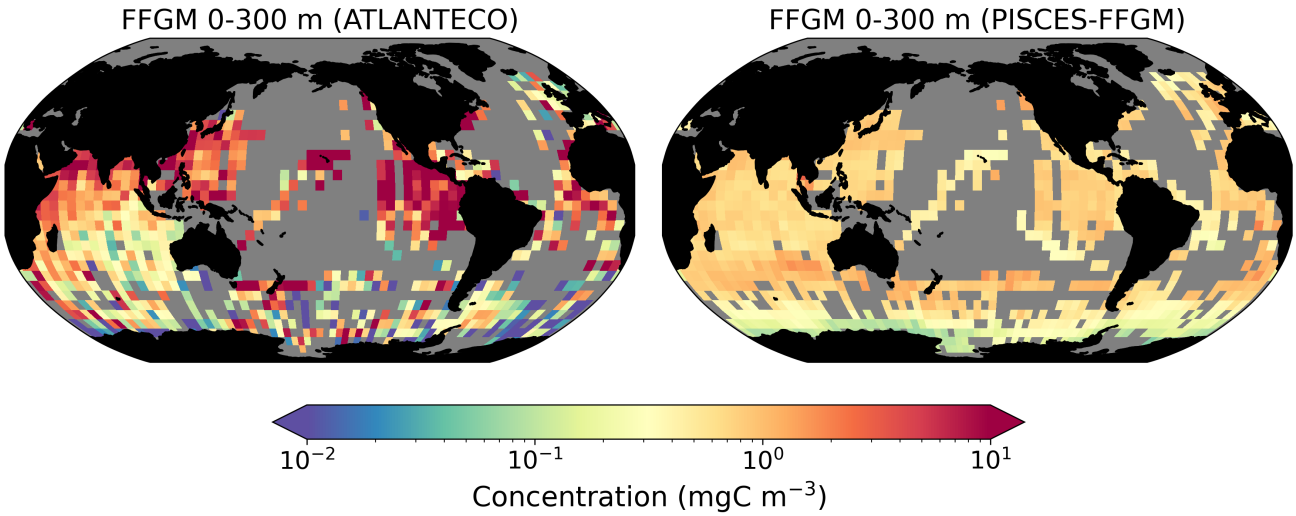

Figure S3. Comparison between AtlantECO observed and PISCES-CLG modeled FFGM biomasses. The colobars are in logarithmic scale. a. Annual average of monthly observations of FFGM concentrations Atlanteco on 5 degree resolution grid. b. Annual average of monthly modeled FFGM concentrations by PISCES-CLG on 5 degree grid masked for missing monthly observations.

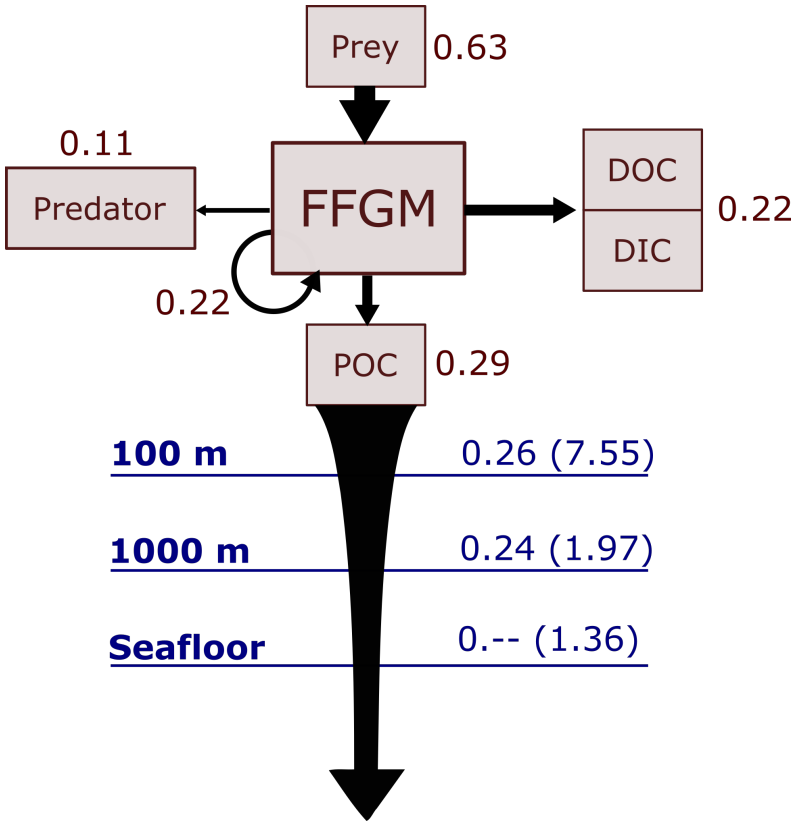

Figure S4. Schematic representation of carbon fluxes induced by processes related to GM. Values are in PgC/year. The upper part of the diagram represents the inflows and outflows of GMs integrated globally over the first 100 meters. The inflow is the grazing on the different prey. The arrow going from GM to GM corresponds to the flux related to growth due to assimilated food. The outflows are : i) the remineralization/non-assimilation processes that go into the dissolved organic carbon (DOC) and dissolved inorganic carbon (DIC) ii) the quadratic and linear mortality terms (directly remineralised in PISCES-FFGM because of the lack of explicit representation of upper level predators) and iii) the production of particular organic carbon (POC) via carcasses and fecal pellets. The lower part of the diagram corresponds to the export of POC linked to the fall of carcasses and fecal pellets of GM. The values in blue correspond to the global annual GM-driven POC flux through the corresponding depth, the values in parenthesis representing the total POC flux (related to FFGM, GM, bPOC and sPOC).

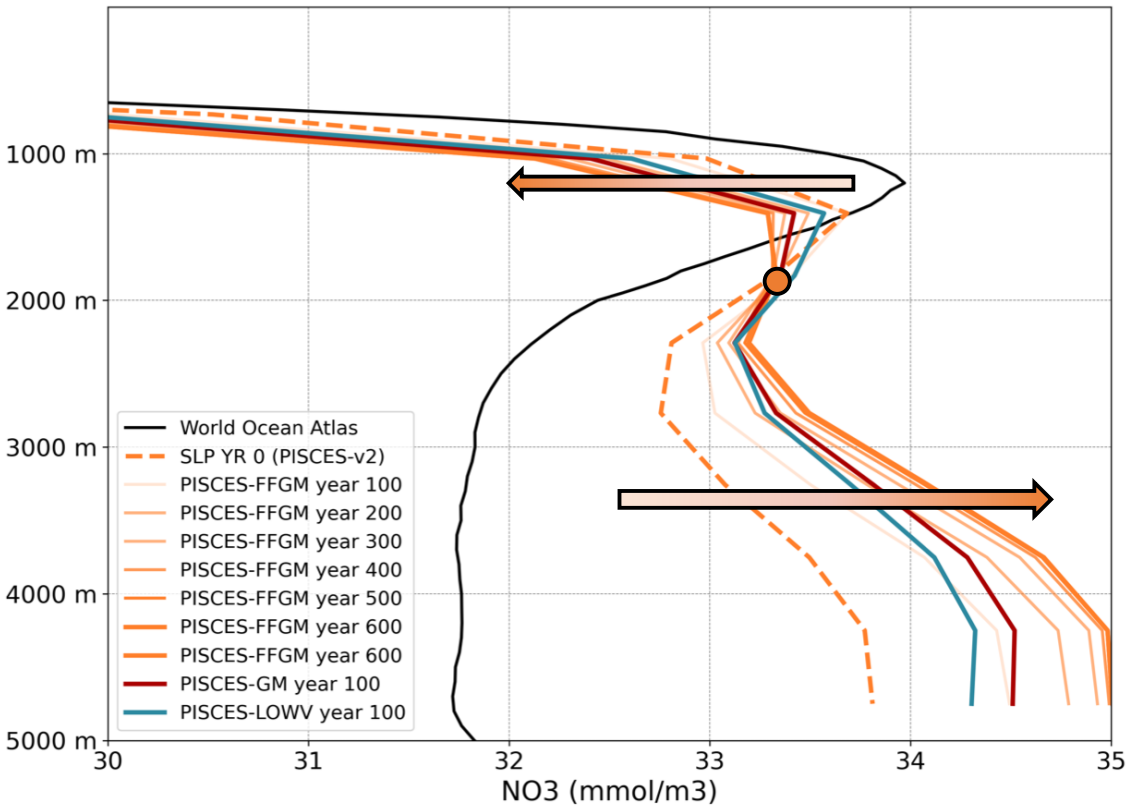

Figure S5. Nutrient profiles drift Globally averaged vertical profile of nitrate concentrations for the PISCES-FFGM model in orange shading, over 600 years of runs. And for the PISCES-LOWV and PISCES-GM models over 100 years of runs starting from year 500 of PISCES-FFGM (in blue and red). In black are the WOA (Garcia et al., 2019) data. In dotted line the PISCES-v2 reference run after 500 years. The shaded arrows indicate the drift direction for the PISCES-FFGM model.

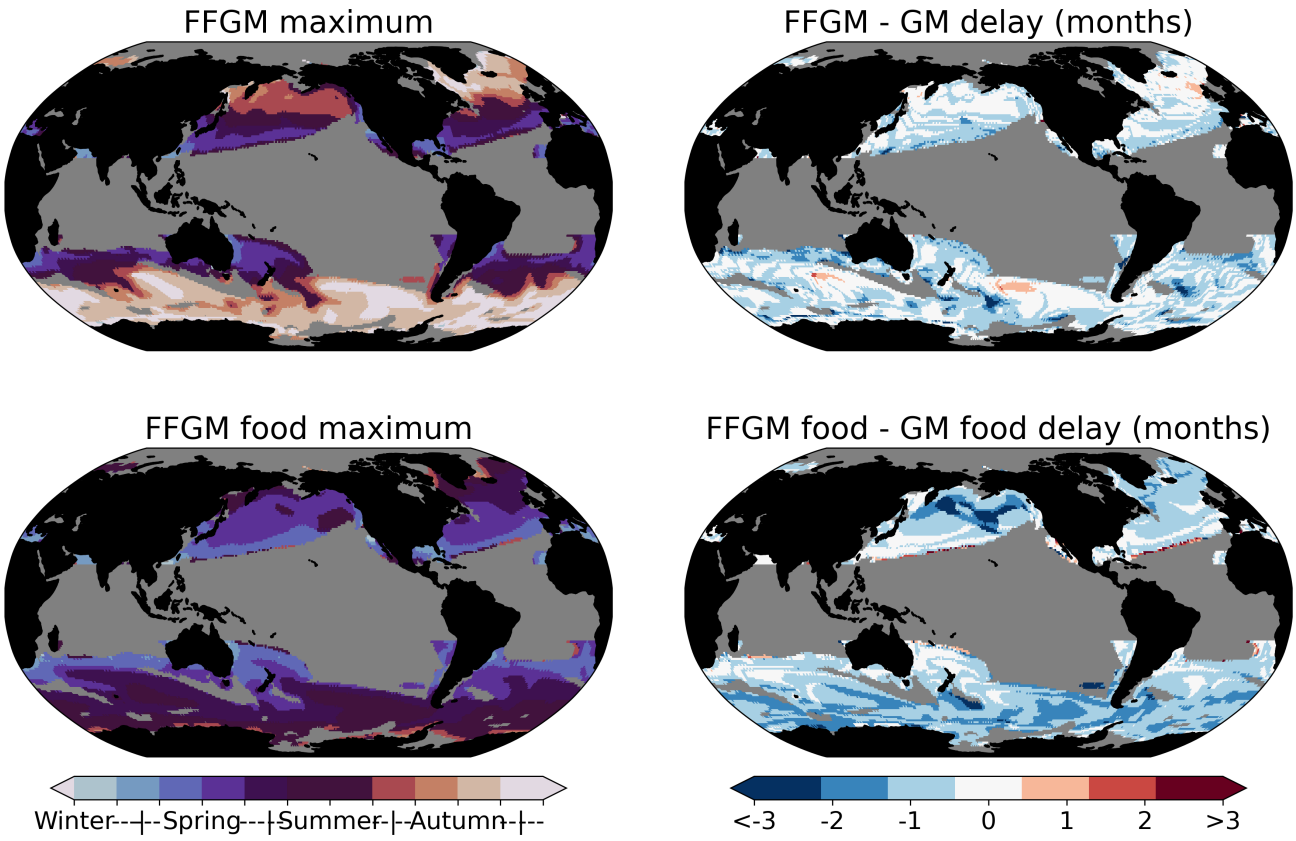

Figure S6. Spatial distribution of the annual period of maximum macrozooplankton biomasses and maximum food availability A filter was applied to keep only the areas at more than 20°latitude from the equator and in which the amplitude of annual biomass variation is higher than 20%. The amplitude is calculated as $(2 \times (max - mix)/(min + max))$ with min the minimum annual biomass and max the maximum annual biomass. a. Map of months with maximal FFGM biomasses b. Map of lag (in months) between months of maximal FFGM biomasses and months of maximal FFGM biomasses c. Map of months with maximal FFGM food availability (calculated as the sum of prey weighted by FFGM preferences for each prey) d. Map of lag (in months) between months with maximal FFGM food availability and months with maximal GM food availability.